Characterization of Alkylating Versus Intercalating Anticancer Drug-Induced Effects on Cell Survival, Cell Cycle Kinetic and Morphonuclear Pattern of Three Neoplastic Cells Lines Growing *in Vitro*

Olivier Pauwels,[1,2] Robert Kiss,[2,4] Jean-Lambert Pasteels,[2] and Ghanem Atassi[1,3]

Received November 15, 1994; accepted February 10, 1995

Purpose. The influence of three alkylating and three intercalating anticancer drugs on cell survival, cell cycle kinetics and chromatin patterns was monitored *in vitro* on three neoplastic cell lines. ***Methods.*** This monitoring was carried out by means of the digital cell image analysis of Feulgen-stained nuclei. ***Results.*** Results show that in term of cytotoxicity, the intercalating drugs were more potent than the alkylating ones. As for the cell kinetics assessment, most of the experimental conditions led to a blockage of the cells in the G_2 phase of the cell cycle. A study of chromatin patterns by means of digital cell image analysis enabled us to describe 15 morphonuclear parameters. The results show that the drugs tested induced specific morphonuclear modifications, e.g. an increase in nuclear size. The 15 morphonuclear parameters were submitted to multivariate analyses, i.e. principal-components analyses followed by the canonical transformation of the data. The results of these multivariate analyses enabled us to discriminate between the alkylating and the intercalating drugs. ***Conclusions.*** We conclude that it would be possible to "diagnose" the mechanism of action of DNA interacting agents (alkylating or intercalating drugs) by means of the combination of digital cell image and multivariate analysis.

KEY WORDS: cell cycle kinetics; chromatin patterns; intercalating drugs; alkylating drugs; cancer pharmacology.

INTRODUCTION

According to Waring (1), since most aspects of the cancer problem revolve around the behavior of DNA, the subject of anticancer drug-DNA interactions has retained the attention of a lot of researchers. Of the anticancer drugs which react with the DNA of neoplastic cells, alkylating and intercalating agents are among the most potent. However, it is often very difficult to distinguish between these two classes of agents on the sole basis of their chemical structures. The fact nevertheless remains that the early identification of the mechanism of action of an anticancer drug is of great importance during the pharmacological evaluation of the drug's activity because this mechanism of action will dictate the toxicological profile of the compound. Indeed, by way of an example, many of the clinically active antineoplastic intercalating drugs are cardiotoxic (2) while most of their alkylating homologues are hematotoxic (3). Thus, in the pharmacological evaluation of a compound it is very important to identify as early as possible whether the compound is an alkylating or an intercalating agent since the clinical management will be completely different. At present, the pharmacological action of alkylating and intercalating drugs is mainly studied by means of alkaline elution methods, which reveal the DNA crosslinking ability of alkylating agents (4), and the single and double strand breaks caused by intercalating ones (5). In our laboratory, we have been interested for a number of years in the digital cell image analysis of anticancer-induced effects on neoplastic cells (6–10). This methodological approach is also used by other research groups (11–13). These studies show that the computerized analysis of Feulgen-stained nuclear images makes it possible to study antineoplastic drug-induced effects on several levels, i.e. cell proliferation (7), cell kinetics (7,9,10,13), and chromatin conformation (7–13).

The aim of the present work is to study the effects of three alkylating and three intercalating anticancer drugs on these distinct levels of drug-induced effects on the biological properties of neoplastic cells (i.e. cell proliferation, cell kinetics, and chromatin conformation) in order to distinguish between alkylating and intercalating drugs. To this end, three neoplastic cell lines, i.e. the MXT mouse mammary cell line (14) and the J82 (15) and T24 (16) human bladder lines, were submitted to the three alkylating drugs (melphalan (L-PAM), a nitrogen mustard; carmustine (BCNU), a nitrosourea; and thiotepa (TT), an ethyleneimine derivative) and the three intercalating drugs (doxorubicin (DOX), an anthracycline; actinomycin D (ACT), a polypeptide linked to a phenoxazone ring); and ellipticine (ELL), an intercalating alkaloid). The effects of these six drugs on cell cycle kinetics and morphonuclear features were studied by means of the digital cell image analysis of Feulgen-stained nuclei. Furthermore, multivariate analyses (principal components analysis with the canonical transformation of the data) of the morphonuclear effects observed were carried out in order to distinguish between alkylating and intercalating drugs. These analyses were carried out according to a methodology previously described in detail (7,9,10).

MATERIALS AND METHODS

Drugs

The melphalan came from Sigma Chemical Co. (St. Louis, USA); the carmustine came from Bristol (Paris La Défense, France); the thiotepa, actinomycin D and ellipticine were obtained from Pierre Fabre Médicaments (Castres, France) and the doxorubicin came from Farmitalia Carlo-Erba (Nivelles, Belgium). The purity of these six drugs was at least 95%.

[1] Laboratoire de Pharmacologie Cellulaire, Institut de Pharmacie, Université Libre de Bruxelles, Boulevard du Triomphe, 1050 Brussels, Belgium.
[2] Laboratoire d'Histologie, Faculté de Médecine, Université Libre de Bruxelles, 808 route de Lennik, 1070 Brussels, Belgium.
[3] Division de Cancérologie, Institut de Recherche Servier, 14 rue de la République, 92150 Suresnes, France.
[4] To whom correspondence should be addressed at Laboratoire d'Histologie (CP 620), Faculté de Médecine, Université Libre de Bruxelles, 808 route de Lennik, 1070 Brussels, Belgium.

Cell Culture

The MXT cell line is a derivative of the murine MXT mammary adenocarcinoma (17). The J82 and T24 human bladder cell lines came from the American Type Culture Collection (Rockville, USA) (HTB1 and HTB4 respectively). The cells were cultured at a temperature of 37°C in an atmosphere containing 5% of CO_2. The culture medium consisted of Eagle's Minimum Essential Medium supplemented with 5% fetal calf serum (decomplemented by 1 hr's processing at 56°C), L-glutamine and antibiotics (all the constituents were from Gibco, Paisley, UK).

Preparation of Samples

The preparation of the samples was similar to that already described (7). Briefly, aliquots of 2.5 ml of a suspension containing 25,000 cells in the exponential growth phase were plated in Petri dishes with a diameter of 35 mm (Nunc, Roskilde, Denmark); in each dish there was a glass microscope coverslip. After 24 hrs' incubation, the medium was supplemented with nine concentrations of each of the 6 antineoplastic drugs studied. Control conditions (CT) included cells cultured in the absence of any drug. After 72 hrs in these experimental conditions, the microscope glass coverslips were fixed in a mixture of ethanol 96% (75 ml), formol 40% (20 ml) and acetic acid 100% (5 ml) (EFA), and mounted on microscope slides by means of DPX (BDH Chemicals, Poole, UK). The slides were stained by means of the Feulgen reagent (Fluka, Buchs, Switzerland) after hydrolysis in 6N HCl for 1 hr at 24°C (18). These slides were used to study drug-induced alkylating and intercalating effects on the growth, the kinetics and the morphonuclear features of cells. Each experimental condition was executed in triplicate.

Cell Growth Assessment

As previously described (9,10), the number of Feulgen-stained cell nuclei present on an area of 16 mm^2 was recorded for each slide subjected to analysis. This assessment was carried out using a microscope (40× magnification lens) equipped with a 100-case grid. Five areas were analysed per slide, and so 15 areas per experimental condition. The values so obtained permitted the assessment of the cytotoxic effect of the drugs on the proliferation of the cell lines in the different experimental conditions.

Cell Kinetic Assessment

The assessment of the proportion of cells in the various phases of the cell cycle was carried out by means of stepwise linear discriminant analysis with reference to specific "morphonuclear data banks" relating to the G_0-G_1, S, G_2 and M phases of the cell cycle. These three data banks were obtained by means of principal components analysis followed by the canonical transformation of the data using a methodology previously described (6,7). The specific "morphonuclear data banks" were set up on the basis of the 15 morphonuclear parameters calculated by means of digital image analysis.

Image Analysis

Three hundred cell nuclei were analysed for each slide by means of a SAMBA 2005 system (Alcatel-TITN, Grenoble, France), so enabling each of the nuclei analysed to be characterized according to 15 morphonuclear parameters (18). Nine hundred cell nuclei were thus computed for each experimental condition studied. These 15 parameters belong to four different algorithms. The first generates one geometric parameter. The second is based on the distribution of the optical density in the nucleus, and groups five densitometric parameters including the integrated optical density (IOD), which corresponds to the DNA content. Five parameters are computed on the basis of the length section matrices (19) and the four remaining ones are computed on the basis of the co-occurrence matrices (20). These 15 parameters are described in Table I. Briefly, except for the nuclear area parameter (which gives the nuclear size) and the integrated optical density (which corresponds to the DNA content), these parameters describe the chromatin texture of the nuclei.

Statistical and Mathematical Analyses

The assessment of cell growth, cell kinetics and the morphonuclear effects of the drugs are reported as means ± standard error of the mean. The statistical comparisons were made by means of the Fisher test.

We also used principal-components analysis followed by the canonical transformation of the data in order to characterize "typical" cell nuclei from the different nuclear populations, i.e. the populations submitted to the different drugs. Such analyses correspond to the multivariate analysis described by Bartels (21). This author reports that multivariate methods are appropriate to describe any differences between cells or any gradual change serving to establish statistical significance of a change. They also serve to discriminate between cells with different properties (21).

RESULTS

Drug-Induced Effects on Cell Survival

In Fig. 1 the open squares depict the survival of the J82 cells in the different experimental conditions. Similar curves were obtained by means of the MXT and T24 cell lines (data not shown). On the basis of such curves it is possible to extrapolate the value of the concentration inhibiting 50% of the cell proliferation (IC50). These values are given in Table II. The results listed in Table II show that the three alkylating agents induced a 50% inhibition in cell proliferation at concentrations ranging between 10^{-6}M and 10^{-4}M. In contrast, the three intercalating agents induced IC50 at concentrations ranging between 10^{-9}M and 10^{-6}M. Thus, the intercalating agents appear to be more potent in terms of cytotoxicity than the alkylating ones.

Drug-Induced Effects on the Cell Cycle

In Fig. 1, the black squares give the effects of the six antineoplastic agents studied on the percentage of J82 cells present in the G_2 phase of the cell cycle. It should be emphasized that a given drug-treated cell nuclei population was

Table I. List of the 15 Morphonuclear Parameters[a]

	Abbreviation	Morphonuclear parameter	Biological relevance
Geometric parameter			
1	NA	Nuclear area	Nuclear size
Densitometric parameters			
2	IOD	Integrated optical density	DNA content
3	MOD	Mean optical density	Chromatin texture
4	SK	Skewness index	Chromatin texture
5	VOD	Variance of the optical density	Chromatin texture
6	K	Kurtosis index	Chromatin texture
Parameters computed on the basis of the length section matrices			
7	SRL	Short run length emphasis	Chromatin texture
8	LRL	Long run length emphasis	Chromatin texture
9	GLD	Gray level distribution	Chromatin texture
10	RLD	Run length distribution	Chromatin texture
11	RLP	Run length percentage	Chromatin texture
Parameters computed on the basis of the co-occurence matrices			
12	LM	Local mean	Chromatin texture
13	E	Energy	Chromatin texture
14	CV	Coefficient of variance	Chromatin texture
15	C	Contrast	Chromatin texture

[a] For each morphonuclear parameters, Table I gives its rank, its abbreviation, its name and its biological relevance.

taken into consideration for G_2 percentage determination when at least 15% of the cells were still present after treatment as compared to the control condition (= 100%). Below this 15%, the number of cells was too low to make morphonuclear analysis possible. The results show that both the alkylating and the intercalating drugs induced a significant increase in the percentage of cells in the G_2 phase. This G_2 phase increase was inversely correlated with the percentage of surviving cells. At the highest concentrations investigated a plateau was sometimes reached with respect to the proportion of cells present in the G_2 phase. Similar results were observed with the MXT and T24 cell lines (data not shown).

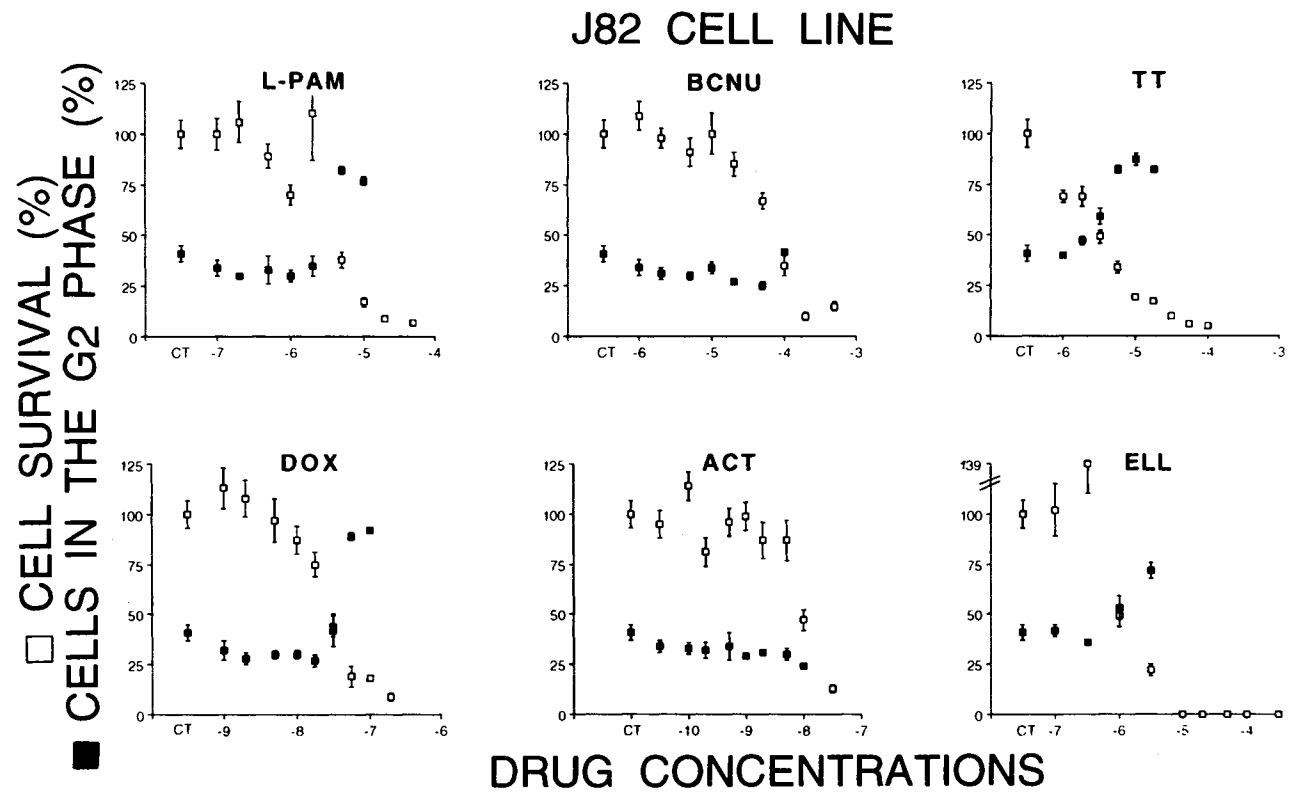

Fig. 1. Cell survival (open squares) obtained with the J82 cell line after 3 days' incubation in the presence of each of the drugs studied, together with the percentage of cells in the G_2 phase of the cell cycle (black squares). The results are expressed in percentages in comparison with the control cells (= 100%) ± standard error of the mean.

Table II. IC50 Values of Alkylating and Intercalating Drugs[a]

	MXT cell line	J82 cell line	T24 cell line
Melphalan	−5.8 ± 0.7	−5.4 ± 1.1	−5.6 ± 0.7
Carmustine	−4.6 ± 0.5	−4.1 ± 0.6	−4.2 ± 0.8
Thiotepa	−5.2 ± 0.6	−5.5 ± 0.3	−5.5 ± 0.7
Doxorubicin	−7.6 ± 1.8	−7.6 ± 1.4	−7.7 ± 1.1
Actinomycin D	−8.5 ± 1.2	−8.0 ± 0.9	−8.4 ± 0.8
Ellipticine	−6.3 ± 1.0	−6.0 ± 0.6	−6.0 ± 1.1

[a] List of the drug concentrations inhibiting 50% of the cell proliferation (IC50) in the three cell lines studied. The results are expressed as the logarithm of the IC50 ± standard error on the mean.

When a significant G_2 phase increase occurred, this increase led to a concomitant decrease in the percentage of cells present in the G_1 phase of the cell cycle (data not shown). Concerning the percentage of cells present in the S and M phases of the cell cycle, no significant modifications were observed in comparison with the control conditions (data not shown).

Drug-Induced Effects at Morphonuclear Level

Taking monovariate analysis as a means of illustrating the morphonuclear effects induced by the alkylating and intercalating drugs, Fig. 2 shows the development of nuclear size (quantitatively described by the nuclear area) in relation to the drug concentrations. As for Fig. 1, only the experimental conditions were analysed for which a significant proportion of the cells (≥15% as compared to the control) were still present, so making digital cell image analysis possible. The results show that nuclear size increased concomitantly with the drug concentrations. Nevertheless, actinomycin D produced no significant ($p > 0.05$) effects on the development of the mean nuclear size value, or only a weak but nevertheless significant ($p < 0.05$ to $p < 0.001$) decrease in this mean value in the case of the T24 cells treated by concentrations of actinomycin D ranging from 10^{-9}M to 10^{-8}M.

Since 15 morphonuclear parameters were taken into consideration in the present study, we would have illustrated the drug-induced effects at morphonuclear level by means of 15 figures, as in Fig. 2, if we had used monovariate analysis. This was not feasible. Due to this fact, these large amounts of information were combined and described by means of multivariate analysis in order to take the 15 morphonuclear parameters into account in one single calculation step. The multivariate analysis employed involved principal-components analysis. This mathematical analysis of data allows a projection into a 2-dimensional space of the 15-dimensional space corresponding to the multiparametric image featuring the 15 parameters computed on each nucleus. This transformation of a 15-dimensional space into a 2-dimensional space is made possible by means of the canonical transformation of the data. This 2-dimensional space is delimited by canonical functions. Each canonical function is a linear combination of the 15 parameters and is uncorrelated with any other. Each of these canonical functions yields part of the information obtained by means of the 15 parameters. By definition, the largest part is yielded by the first canonical function. The second canonical function is the next most

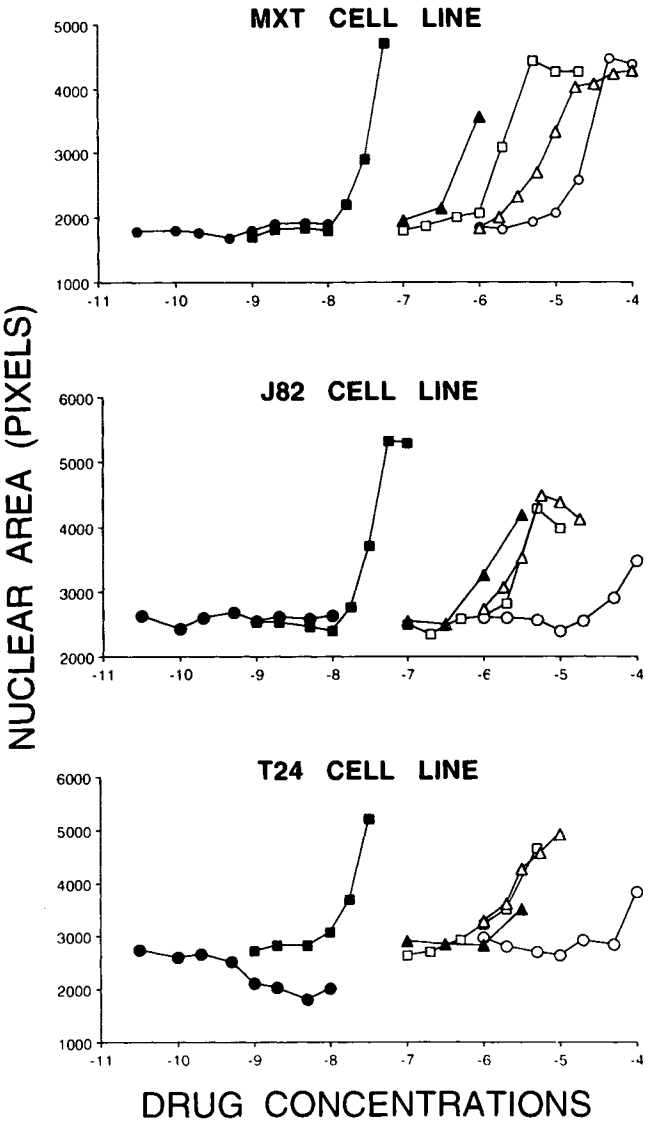

Fig. 2. Development of the nuclear area (NA) in the different experimental conditions tested. The open symbols show the effects of the 3 alkylating agents (melphalan = open squares, carmustine = open circles, thiotepa = open triangles). The black symbols show the effects of the intercalating agents (doxorubicin = black squares, actinomycin D = black circles, ellipticine = black triangles). The standard errors of the mean are not shown because they do not emerge from the symbols.

important one, and so on. So the plane described by the first two canonical functions is the most potent canonical plane in terms of the quantity of information given. In the present work, the first two canonical functions gave at least 85% of the total information. In other words, these first two canonical functions explain at least 85% of the variance between the factorial cell distributions corresponding to the different experimental conditions. This is the reason why we chose to represent only the planes describing the first two canonical functions (Figs. 3 and 4). Because it is not possible to represent on a factorial plane each of the 900 cell nuclei for each of the 30 drugs studied, Figs. 3 and 4 depict only the 95% confidence interval around the mean position of each of the

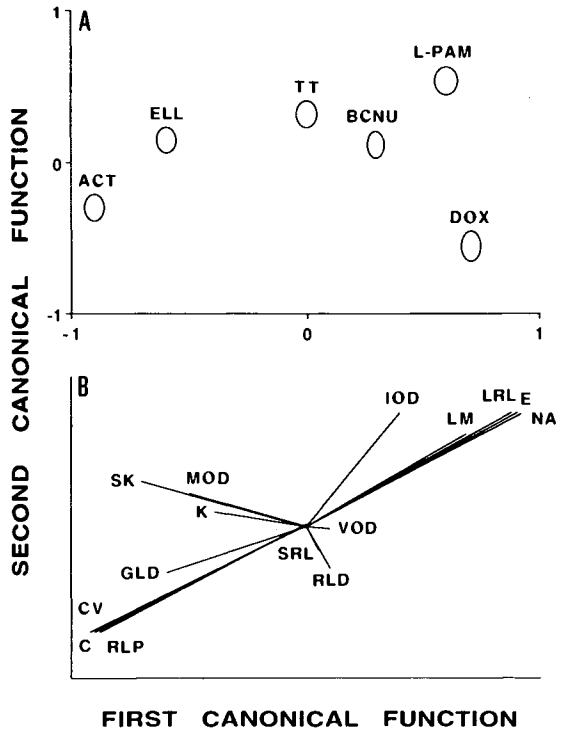

Fig. 3. Multivariate analysis performed with the J82 cell line on the basis of the values of the 15 parameters described by means of digital cell image analysis. The experimental conditions used for this mathematical analysis were those corresponding to the concentrations inhibiting between 51 and 65% of the cell proliferation. This multivariate analysis made it possible to locate each drug (symbolized by an ellipsis corresponding to the 95% confidence interval of the mean position of the factorial cell distribution of the treated nuclei) in a 2-dimensional space by means of the canonical transformation of the data (Fig. 3A). The canonical projection of the 15 parameters is represented in front of each factorial distribution (Fig. 3B) in order to indicate the direction and strength of the parameter scattering of the cell populations under analysis.

factorial cell distributions corresponding to each of the experimental conditions.

Fig. 3 gives the results obtained by means of a this multivariate analysis. This analysis was performed for the J82 cell line on the basis of the morphonuclear characteristics obtained for 900 cell nuclei whose digitized nuclear images were merged into one file. For this multivariate analysis (illustrated in Fig. 3), we employed only one concentration of each drug studied, i.e. the drug concentration inducing a 50% inhibition in the cell proliferation (IC50) (in fact, the concentration which is the nearest to the IC50 values). So we used the following experimental conditions: melphalan at a concentration of $10^{-5.3}$M, carmustine at a concentration of $10^{-4.0}$M, thiotepa at a concentration of $10^{-5.5}$M, doxorubicin at a concentration of $10^{-8.0}$M, actinomycin D at a concentration of $10^{-8.0}$M and ellipticine at a concentration of $10^{-6.0}$M. These concentrations corresponded to a cell proliferation of between 35% and 49% of the cell proliferation of the control cells. Fig. 3 shows the results of the principal-components analysis performed on the basis of these six experimental conditions. In Fig. 3A, each ellipsis corresponds to the 95% confidence interval around the mean position of the factorial cell distribution of each experimental condition (i.e., melphalan (L-PAM) at a concentration of $10^{-5.3}$M, carmustine (BCNU) at a concentration of $10^{-4.0}$M, thiotepa (TT) at a concentration of $10^{-5.5}$M, doxorubicin (DOX) at a concentration of $10^{-8.0}$M, actinomycin D (ACT) at a concentration of $10^{-8.0}$M and ellipticine (ELL) at a concentration of $10^{-6.0}$M). These ellipses were placed on a two-dimensional plane circumscribed by the first two canonical functions. The ellipses corresponding to the alkylating agents (L-PAM, BCNU, TT) are located in the upper right-hand superior area of the plane and the intercalating drugs (DOX, ACT, ELL) are dispersed over the rest of it. Fig. 3B makes it possible to assess the descriptive information contributed by each of the 15 parameters (vectors). Indeed, Fig. 3B gives the direction and strength of the parameter scattering for the cell populations under study. In other words, the projection of vectors (corresponding to each of the 15 parameters) on the axes of the first (X axis) and second (Y axis) canonical functions gives the importance of each of these 15 parameters according to the first and second canonical functions respectively. So in the light of Fig. 3B, it emerges that the NA, LRL, RLP, CV and C parameters have the greatest influence on the position of the ellipses in accordance with the first canonical function. On the other hand, the second canonical function is strongly influenced by the NA, LRL, RLP, LM, CV and C parameters. In contrast, the VOD and SRL parameters have little influence in accordance with the first two canonical functions.

In this multivariate analysis, a problem stemming from the use of the experimental conditions corresponding to the concentrations inducing about a 50% inhibition in the cell proliferation is that it is extremely difficult (if not impossible) to obtain this concentration exactly. This is the reason why, in our example in Fig. 3A, the concentrations used in reality inhibited between 65% and 51% of the cell proliferation. At these concentrations, the sigmoids representing the relation between the doses and the morphonuclear effects (see Fig. 2 for example) slope up steeply. This means that for little difference in the concentrations, there are important differences in the mean values of the morphonuclear parameters. This is the second reason why we prefer to study the morphonclear effects of the drugs at the highest concentrations. At these concentrations, the mean values of the morphonuclear parameters develop moderately (see in Fig. 2 the effects of the three alkylating drugs on the development of the nuclear area (NA) of the different cell lines studied). Furthermore these concentrations induce the most marked morphonuclear effects (see Fig. 2). For these reasons, only the highest concentration analysed for each drug was taken into account in the further principal-components analysis.

Figs. 4 A, C and E were drawn up according to the first two canonical functions. Figs. 4 B, D and F make it possible to assess the descriptive information contributed by each of the 15 parameters (vectors). In other words, Figs. 4 B, D and F give the direction and strength of the parameter scattering for the cell populations under study.

Fig. 4 A gives the results for the multivariate analyses carried out on the MXT cells. The results show that the ellipses describing the alkylating agent-induced effects on the MXT cell nuclei are located among the positive values of the first canonical function, and among the negative values of the second one. In contrast, the ellipses describing the

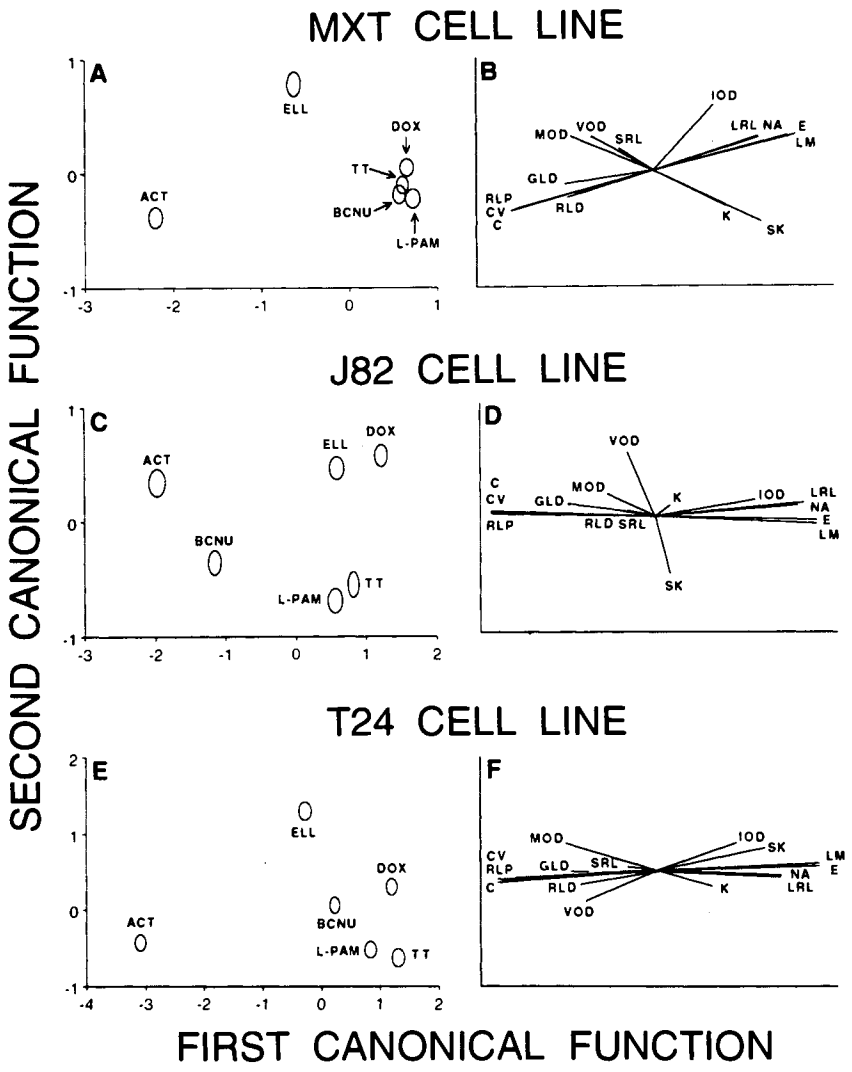

Fig. 4. The legend to Fig. 4 is similar to Fig. 3 but deals with the MXT (Fig. 4A and B), J82 (Fig. 4C and D) and T24 (Fig. 4E and F) cell lines: Figs. 4A, C and E give the location of the 95% confidence interval of the mean position of the factorial cell distribution of the treated nuclei; Figs. 4B, D and F indicate the direction and strength of the parameter scattering of the cell populations under analysis. In contrast to Fig. 3, the experimental conditions used for Fig. 4 correspond to the highest concentrations studied, as justified in the results.

intercalating agent-induced effects on the MXT cell nuclei are located on the three remaining quarters of the plane.

Fig. 4C shows the results obtained by means of multivariate analysis carried out on the J82 cell line. These results show that the ellipses relating to the alkylating agents are situated among the negative values of the second canonical function while those relating to the intercalating drugs are situated among the positive values of this function.

In the case of the T24 cell line (Fig. 4E), the results are similar to those obtained with the MXT line except that the ellipsis corresponding to the carmustine is located among the positive values of the second canonical function and not among the negative ones, as is the case with the MXT cells.

The levels of statistical difference which exist between the positions of the various ellipses are given by means of two values labelled "a:b".The "a" value represents the percentage of "well-classified nuclei" as assessed by means of non-supervised stepwise linear discriminant analysis. The "b" value corresponds to the F value of the Fisher test calculated for the most discriminatory parameter. All these "a:b" values corresponding to each pair of drugs are statistically significant. For example, the "a:b" values obtained in the case of the MXT cell line by the comparison of the carmustine-treated cells with thiotepa-treated ones are "56: 11". These values corresponds to a statistical level of significance corresponding to $p < 0.01$. In all the other cases, the level of statistical significance is $p < 0.001$ (data not shown).

Figs. 4B, D and F show that the nuclear area (NA) (the geometric parameter), the long run length emphases (LRL), the run length percentage (RLP) (two parameters computed on the basis of the run length section matrices), and the parameters stemming from the co-occurrence matrices (LM, E, CV and C) were the most important parameters on the

basis of the first canonical function. Indeed, it is these parameters which exhibit the largest projection onto this canonical function, symbolized by the X axis. The densitometric parameters (IOD, MOD, VOD, SK and K) were the most significant parameters with respect to the second canonical function, symbolized by the Y axis.

DISCUSSION

Alkylating and intercalating anticancer drugs possess in common the fact that they act by a binding to the DNA. While alkylating agents act by covalent DNA binding (3), intercalating drugs insert themselves between base DNA pairs (22). The aim of the present work is to investigate whether the digital cell image analysis of Feulgen-stained nuclei can contribute sufficient information to make it possible to distinguish between these alkylating and intercalating agents. In order to validate the methodology used here, the drug-induced alkylating and intercalating effects were also monitored at both cell proliferation and cell kinetics levels.

The results show that with respect to the drug-induced cytotoxic effects (i.e. as they appeared at cell proliferation level), the three intercalating agents acted as lower concentrations than the alkylating agents, at least in our experimental conditions.

With respect to the cell cycle effects, the results show that the drugs lead to a blockage of the cells in the G_2 phase of the cell cycle (except for actinomycin D). This feature has been previously described (23). Since both alkylating and intercalating drugs lead to the same effect (i.e. an accumulation of the cells present in the G_2 phase), it is not possible to distinguish between these two pharmacological classes of anticancer drugs on the basis of their cell cycle effects. This is the reason why we went further in our investigations and used multivariate analysis, which describes the drug-induced alkylating and intercalating effects at morphonuclear level. We used this methodological approach because our working hypothesis is as follows. Since alkylating agents induce DNA crosslinking (3,4) while intercalating agents induce DNA strand breakage (5,24), it is logical to believe that their effects at morphonuclear level would be different. In other words, the analysis of the morphological aspect of cell nuclei treated by alkylating and intercalating drugs would made it possible to ascertain the mechanism of action of a DNA-interacting drug. We made use of the multivariate analysis of Feulgen-stained nuclei in order to verify this hypothesis. This multivariate analysis took into account 15 parameters quantitatively (and thus objectively and reproducibly) describing nuclear characteristics relating to geometric, densitometric and textural features (18). This multivariate analysis made it possible to distinguish between the six drugs according to their mechanisms of action. Regarding the MXT cell line, alkylating agents occupied a specific position on the plane described by the first two canonical functions, i.e. among the positive values of the first canonical function and among the negative values of the second one. In contrast, the intercalating drugs were located on the other parts of the factorial plane. A similar observation was made in the case of the T24 cell line. As for the J82 cell line, the intercalating drugs were located among the positive values of the second canonical function while the alkylating drugs were located among the negative ones. The results illustrated in Fig. 4 show that the part of the plane occupied by the intercalating drugs is larger than the one occupied by the alkylating agents. This observation might be explained, at least partly, by the fact that in contrast to alkylating drugs, intercalating ones act on the basis of more than one operating mechanism. Indeed, intercalating agents act not only through DNA intercalation but also through topoisomerase II inhibition (25). In addition to these two mechanisms of action, doxorubicin is also able to act via the formation of free radicals, via covalent DNA binding and via action against the cell membrane (26). It is also possible that doxorubicin acts via topoisomerase I inhibition (27). The present study shows that a rule seems to emerge from the multivariate analyses. Indeed, these multivariate analyses similarly located the intercalating agents on the basis of the first canonical function whatever the cell line. Indeed, the actinomycin D was located among the negative values of this function, the ellipticine was located in the middle values, and the doxorubicin among the positive ones. The location of the doxorubicin was similar to the locations of the alkylating agents (except in the case of the J82 cell line). This similarity between doxorubicin and alkylating drugs may be due to the fact that doxorubicin may also act by covalent DNA binding (26) in the same way as alkylating agents.

Of course, our methodology has its limitations. Indeed there are anticancer drugs which do not have any significant effects on cells' morphonuclear features. For example, in the present study the actinomycin D had no significant effects on the morphonuclear parameters studied (as demonstrated by its effects on nuclear size and cell cycle kinetics). This observation may be explained by the fact that the most important biochemical effects of the DNA intercalation of actinomycin D are the inhibition of RNA and, secondarily, protein synthesis (28). Furthermore, this methodology gives the "mean morphonuclear-induced effect" of the antineoplastic drugs tested. So, as mentioned above, doxorubicin acts through a series of mechanisms of action. Digital cell image analysis gives only the resulting morphonuclear effect of this drug. This is probably the reason why doxorubicin is recognized as being either an intercalating or an alkylating drug. Lastly, if the use of "principal-components analysis" enables the mechanism of action of a new (i.e. investigational) drug to be identified by reference to well-known anticancer drugs, it will be difficult (if not impossible) to ascertain the mechanism of action of a drug possessing an original one. So, digital image analysis must be considered as a test enabling the mechanism of action of a drug to be rapidly presumed, but the result obtained must be validated by more conventional methods.

In conclusion, the results of the present work show that in terms of cytotoxicity, intercalating agents are more potent than alkylating ones. In terms of cell cycle kinetics, both alkylating and intercalating drugs induce a G_2 cell arrest. However, the information contributed by the combination of the cell proliferation rule and the cell cycle kinetics assessments did not make it possible to distinguish between the alkylating and the intercalating drugs. This was rendered possible by the use of multivariate analysis taking into account 15 morphonuclear parameters computerized by means

of computer-assisted microscope analysis on Feulgen-stained nuclei. It therefore appears that the present study offers a new pharmacological method that makes it possible to characterize the mechanism of action of a given drug for which an alkylation or intercalation mechanism is presumed to exist. Applied to investigational agents, this methodology seems to permit the rapid identification of the mechanism of action of a potential new anticancer drug. The ultimate goal of these experiments consists of the establishment of a "map" corresponding to the factorial plane on which it will be possible to identify antineoplastic drugs on the basis of their position on this "map" and according to their operating mechanisms. The "map" that we are currently drawing up will include not only alkylating and intercalating drugs, but also antimetabolite, antimitotic and other drug types.

ACKNOWLEDGMENTS

O.P. is the holder of a grant from the "Fonds National de la Recherche Scientifique" (F.N.R.S., Belgium) and R.K. is a Research Associate with the F.N.R.S., Belgium.

REFERENCES

1. Waring M. J. DNA modification and cancer. *Ann. Rev. Biochem.* 50:159–192 (1981).
2. C. E. Myers and B. A. Chabner. Anthracyclines. In: B. A. Chabner and J. M. Collins (eds.) *Cancer chemotherapy: principles and practice,* Lippincott Company, Philadelphia, 1990, pp. 356–381.
3. M. Colvin and B. A. Chabner. Alkylating agents. In: B. A. Chabner and J. M. Collins (eds.) *Cancer chemotherapy: principles and practice,* Lippincott Company, Philadelphia, 1990, pp. 276–313.
4. A. Sunters, C. J. Springer, K. D. Bagshawe, R. L. Souhami, and J. A. Hartley. The cytotoxicity DNA crosslinking ability and DNA sequence selectivity of the aniline mustards melphalan chlorambucil and 4-[bis(2-chloroethyl)amino] benzoic acid. *Biochem. Pharmacol.* 44:59–64 (1992).
5. W. E. Ross and M. C. Smith. Repair of deoxyribunucleic acid lesions caused by adriamycin and ellipticine. *Biochem. Pharmacol.* 31:1931–1935 (1982).
6. C. Etiévant, O. Pauwels and R. Kiss. Digital cell image analysis of verapamil-induced effects in chemosensitive and chemoresistant neoplastic cell lines. *J. Cancer Res. Clin. Oncol.* 120:76–84 (1993).
7. O. Pauwels and R. Kiss. The application of computerized analysis of nuclear images and multivariate analysis to the understanding of the effects of antineoplastic agents and their mechanism of action. *Methods Find. Exp. Clin. Pharmacol.* 15:113–124 (1993).
8. O. Pauwels and R. Kiss. Monitoring of chemotherapy-induced morphonuclear modifications by means of digital cell image analysis. *J. Cancer Res. Clin. Oncol.* 119:533–540 (1993).
9. O. Pauwels, R. Kiss, and G. Atassi. Computer-assisted microscope analysis of morphonuclear modifications induced by anticancer antimetabolites in cell lines cultured in vitro. *Anti-Cancer Drugs* 5:160–170 (1994).
10. O. Pauwels, G. Atassi, and R. Kiss. Combination of computerized morphonuclear and multivariate analyses to characterize in vitro the antineoplastic effect of alkylating agents. *J. Pharmacol. Toxicol. Methods,* 33:35–45 (1995).
11. M. Briffod, F. Spyratos, M. Tubiana-Hulin, C. Pallud, C. Mayras, A. Filleul, and J. Rouëssé. Sequential cytopunctures during preoperative chemotherapy for primary breast carcinoma. Cytomorphologic changes initial ploidy and tumor regression. *Cancer* 63:631–637 (1989).
12. M. Briffod, F. Spyratos, K. Hacène, M. Tubiana-Hulin, C. Pallud, F. Gilles, and J. Rouëssé. Evaluation of breast carcinoma chemosensitivity by flow cytometric DNA analysis and computer assisted image analysis. *Cytometry* 13:250–258 (1992).
13. E. Colomb, C. Dussert, and P. M. Martin. Nuclear texture parameters as discriminant factors in cell cycle and drug sensitivity studies. *Cytometry* 12:15–25 (1991).
14. R. Kiss, N. Devleeschouwer, R. J. Paridaens, J. C. Heuson, and G. Atassi. Phenotypic change of the transplantable MXT mammary adenocarcinoma into mixed bone producing sarcoma-like tumors. *Anticancer Res.* 6:753–760 (1986).
15. C. O'Toole, Z. H. Price, Y. Ohnuki, and B. Unsgaard. Ultrastructure kariology and immunology of a cell line originated from a human transitional-cell carcinoma. *Br. J. Cancer* 38:64–76 (1978).
16. J. Bubenik, M. Baresova, J. Jakoubkova, H. Sainerova, and J. Donner. Established cell line of urinary bladder carcinoma (T24) containing tumour-specific antigen. *Int. J. Cancer* 11:765–773 (1973).
17. C. Watson, D. Medina, and J. H. Clark. Estrogen receptor characterization in a transplantable mouse mammary tumor. *Cancer Res.* 37:3344–3348 (1977).
18. R. Kiss, I. Salmon, I. Camby, S. Gras, and J. L. Pasteels. Characterization of factors in routine laboratory protocols that significantly influence the Feulgen reaction. *J. Histochem. Cytochem.* 41:935–945 (1993).
19. M. M. Galloway. Texture analysis using gray run lengths. *Comput. Graph. Image Proc.* 4:172–179 (1975).
20. R. M. Haralick, T. Shanmugam, and I. Dinstein. Textural features for image classification. *IEEE. Trans. Syst. Man. Cybern. SMC.* 3:610–620 (1973).
21. P. H. Bartels. Numerical evaluation of cytologic data. V. Bivariate distributions and the bayesian decision boundary. *Anal. Quant. Cytol.* 2:8377–8383 (1980).
22. W. D. Wilson and R. L. Jones. Intercalating drugs: DNA binding and molecular pharmacology. *Adv. Pharmacol. Chemother.* 18:177–222 (1981).
23. B. T. Hill. Cancer chemotherapy. The relevance of certain concepts of cell cycle kinetics. *Biochim. Biophys. Acta* 516:389–417 (1978).
24. W. E. Ross, D. Glaubiger, and K. W. Kohn. Qualitative and quantitative aspects of intercalator-induced DNA strand breaks. *Biochim. Biophys. Acta* 562:41–50 (1979).
25. E. Schneider, Y. H. Hsiang, and L. F. Liu. DNA topoisomerases as anticancer drug targets. *Adv. Chemother.* 27:149–183 (1990).
26. J. Cummings, L. Anderson, N. Willmott, and J. F. Smyth. The molecular pharmacology of doxorubicin in vivo. *Eur. J. Cancer* 27:532–535 (1991).
27. P. D. Foglesong, C. Reckord, and S. Swink. Doxorubicin inhibits human DNA topoisomerase I. *Cancer Chemother. Pharmacol.* 30:123–125 (1992).
28. J. Verweij, J. den Hartigh, and H. M. Pinedo. Antitumor antibiotics. In: B. A. Chabner and J. M. Collins (eds.) *Cancer chemotherapy: principles and practice,* Lippincott Company, Philadelphia, 1990, pp. 382–396.